Int. J. Nano Dimens., 10 (4): 400-409, Autumn 2019

ORIGINAL ARTICLE

Green synthesis, characterization and photo catalytic degradation efficiency of Trimanganese Tetroxide nanoparticle

Gopalakrishnan Nair Sreekala *, Fathimabeevi Abdullakutty, Bhaskaran Beena

Nanoscience Research Lab, Department of Chemistry, KSMDB College, Sasthamcotta, Kollam PIN-690521, Kerala, India.

Received 11 March 2019; revised 16 June 2019; accepted 20 June 2019; available online 26 June 2019

Abstract

Mn_3O_4 nanoparticles has been synthesised from Manganese (II) acetate and Simarouba Glauca leaf extract using microwave heating. This novel method of synthesis of Mn_3O_4 is fast, low-cost, non-toxic and environment friendly. The synthesised product was characterised by powder X-ray diffraction(XRD),Fourier transform infrared spectroscopy(FT-IR), Ultraviolet-Visible spectroscopy(UV-Visible), X-ray photoelectron spectroscopy(XPS), Scanning electron microscopy(SEM) and Transmission electron microscopy(TEM). The prepared material was identified as of tetragonal hausmannite crystalline structure with spherical morphology and particle size 15 nm. Photo catalytic degradation ability of the synthesised product was examined by using it for the degradation of Malachite green dye in various experimental conditions under visible light. The synthesised Mn_3O_4 was found to be an efficient photo catalyst for the removal of Malachite green at the optimum conditions of pH 9, adsorbent dose 0.1 g and dye concentration 20ppm. This study thus reveals the applicability of nanoparticles of Mn3O4 for the removal of pollutants from industrial waste water.

Keywords: *Hausmannite; Microwave Method; Mn_3O_4; Photo Catalyst; Simarouba Glauca.*

How to cite this article

Nair Sreekala G, Abdullakutty F, Beena B. Green synthesis, characterization and photo catalytic degradation efficiency of Trimanganese Tetroxide nanoparticle. Int. J. Nano Dimens., 2019; 10 (4): 400-409.

INTRODUCTION

Different types of hazardous dye effluents are discharged into water bodies by industries like pharmaceutical, food, printing and textiles [1-4]. Dyes like azo dyes, Fluorescein dyes, etc. are highly toxic and carcinogenic. Fluorescein dyes have been reported to be highly cytotoxic for mammalian tissues and they trigger morphological and genetic alterations [5]. Therefore the disposal of organic dyes into water bodies is a matter of concern. Malachite green (MG) is extensively used in many industries as a dye for leather, textiles and also in aquaculture to control fish parasites and diseases. Its use has increased considerably because of its easy preparation and low manufacturing cost.

The removal of dyes from industrial-effluents is a serious problem as these dye molecules are difficult to decompose. Different methods have been implemented for the degradation of dyes in aqueous solution. These include adsorption, biological treatment, advanced oxidation process (AOPS), electrochemical deposition and photo catalysis [6-10]. Of these, photo catalysis has been considered as the cost effective method for the purification of dye containing waste water. For example, the degradation of Rhodamine B dye under visible light irradiation in presence of PbS-sensitized $K_4Nb_6O_{17}$ nanocomposite [11], the degradation of Methylene Blue dye under visible light by MoO_3/Fe_2O_3/rGO ternary nanocomposite [12], and the degradation of Methylene Blue by SnS_2- SiO_2@ α – Fe_2O_3 nanocomposite in presence of visible light [13].

Of the various transition metal oxides, Manganese oxides have generated considerable interest in various fields like catalysis, energy storage, magnetic data storage, drug delivery and biomedical imaging [14]. Mn_3O_4 is mainly used as a source of ferrite materials [15], and applied in various industrial fields such as magnetic [16], electrochemical [17], and catalytic [18, 19].

* Corresponding Author Email: *sreekalamohankumar@gmail.com*

Mn_3O_4 nanoparticles of various size and morphologies are synthesized by methods like chemical bath deposition[20], sol-gel technique[21], co-precipitation[22], solvothermal /hydrothermal synthesis[23], microwave method[24], thermal decomposition[25], vapour phase growth[26],vacuum calcining [27], ultrasonic/gamma irradiation[28-29] and surfactant assisted method[30]. But green synthesis is environment-friendly and economically important compared to the traditional route, which uses toxic organic solvents or precursors [20-30]. In the present study we report the synthesis of Mn_3O_4 by using Simarouba glauca leaf extract. Simarouba glauca is an evergreen tree and has a long history as herbal medicine [31]. Medicinal plants contain a large variety of chemical substances known as secondary metabolites which include alkaloids, steroids, flavonoids, terpenoids, glycoside, saponia, tannins, phenolic compounds and so on. These compounds function as capping agents to regulate the particle size and also as oxidizing or reducing agents [32-33]. Mn_3O_4 synthesized by the above method was well characterized and used as a catalyst in the photo catalytic degradation of malachite green dye.

Spinels are the class of compounds of the type $M^{2+}M_2^{3+}O_4$, which has attracted researches because of their versatile properties and applications in various fields [34]. Mn_3O_4 is a normal spinel with Mn^{2+} in the tetrahedral sites, Mn^{3+} in the octahedral sites and the oxide ions in the cubic close packed arrangement. Mn_3O_4 is one of the most stable oxides of manganese. It is a magnetic material and is an effective and inexpensive catalyst in various oxidation and reduction reactions [36-37]. It is also a direct band gap semiconductor.

EXPERIMENTAL

Materials and Methods

All the chemicals used were of analytical grade and used without any further purification. Manganese (II) acetate tetra hydrate [$(CH_3COO)_2Mn.4H_2O$] was purchased from Merck.

Malachite green ($C_{23}H_{25}N_2Cl$), dye which is mainly used in textile industries was procured from Merck, India. The molecular weight of malachite green is 364.90 g/mol and it absorbs at a maximum wavelength of 620 nm. The chemical structure of the dye is shown in Fig. 1.

Preparation of Simarouba glauca Leaf extracts

Simarouba glauca leaves were collected, washed, dried in shade and pulverized. A definite amount of pulverized leaf was heated with fixed volume of distilled water in a microwave oven at 100W for 30minutes. It was then cooled, filtered and the filtrate was collected.

Synthesis of Mn_3O_4 nanoparticle

60ml of the above filtrate was added drop wise to 50ml of 0.1M Manganese acetate solution with stirring and then heated in a microwave oven at 100W for 15 minutes. The solution was then cooled and the brown precipitate obtained was separated by centrifuging, washed several times with distilled water and ethanol. Finally the product obtained was dried and calcined in a muffle furnace at 500^0C for 2 hour.

Characterization of Mn_3O_4 nanoparticle

The structural identity and phase purity of the prepared material were verified by powder X-ray diffraction technique (XRD) using a Bruker AXS D8 Advance model diffractometer with Cu Kα radiation. FT-IR spectrum was recorded with Fourier transform infrared (FT-IR) spectrometer of Thermo Nicolet, Avatar 370 model. The UV-Visible absorption spectrum of the powder sample was recorded at room temperature using UV-VISIBLE spectrophotometer of model Cary 5000. X-ray photoelectron spectrum (XPS) was performed on

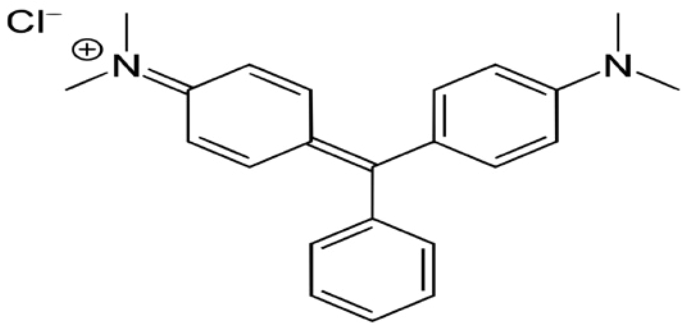

Fig. 1. Chemical Structure of Malachite green.

a K-ALPHASXM Scanning X-microprobe with an Al cathode as the X-ray source. Surface morphology of the sample was analyzed by SEM of JEOL Model JSM - 6390LV. The elemental composition was determined by EDX of model OXFORD XMX N. The particle size and shape were obtained by TEM of model JEOL/JEM 2100.

Photo catalytic Degradation of Malachite Green Dye

A 1000 ppm stock solution of malachite green was prepared by dissolving 1 gm of the dye in 1000 ml distilled water. The absorption maximum of the dye was determined with the help of a UV-Visible spectrophotometer of Model GENESYS 10S.

Photo catalytic degradation efficiency of nano Mn_3O_4 was studied by measuring the absorbance of MG dye solution. Photo degradation experiments were carried out by using the dye solution of concentration 10ppm prepared using distilled water. A known dose (0.05gm) of the photo catalyst, Mn_3O_4, was added in to the beaker containing 200ml of the dye solution and the mixture was stirred in the dark for 30 min to establish an adsorption-desorption equilibrium. The reaction mixture was then exposed to sunlight for 150 minutes. A small portion of the dye was withdrawn at regular intervals (30mins.) and the concentration of dye in each degraded sample was determined by measuring the absorbance of the dye with UV-Visible spectrophotometer. The experiments were repeated with different concentrations of the dye [20, 30 & 40 ppm], different amounts of photo catalyst [0.1, 0.15, & 0.2 gm] and different pH [3, 5 & 9]. The pH of the solution was measured by a digital pH meter and the desired pH was adjusted by the addition of 0.1N sodium hydroxide or 0.1N hydrochloric acid.

The percentage of degradation was determined by using the following equation,

$$\text{Removal (R \%)} = [\frac{(C0 - Ce)}{C0}] * 100 \quad (1)$$

where R% is the degradation efficiency of Mn_3O_4, C_0 [mg/L] and C_e [mg/L] are initial and equilibrium concentrations of MG in aqueous solution at different reaction time [38].

RESULTS AND DISCUSSION

Colour and appearance

Nanoparticles of Mn_3O_4 were obtained as a coffee brown coloured fine powder.

Powder X- ray diffraction technique

XRD peaks give the phase purity, structural identity and particle size of the prepared nanomaterial. The powder XRD pattern of the synthesized product (Fig. 2) matched well with JCPDS Card No. 24-0734 and all diffraction peaks were indexed to the tetragonal hausmannite structure. Particle size calculated using Debye-Scherer equation was found to be nearly 15nm. No peaks from other phases were found, suggesting the high purity of the synthesized Mn_3O_4 nanoparticles.

FT-IR spectroscopy

FT-IR spectrum of the sample is given in Fig. 3. FT-IR spectrum is used to identify the various bond types and functional groups present in the product

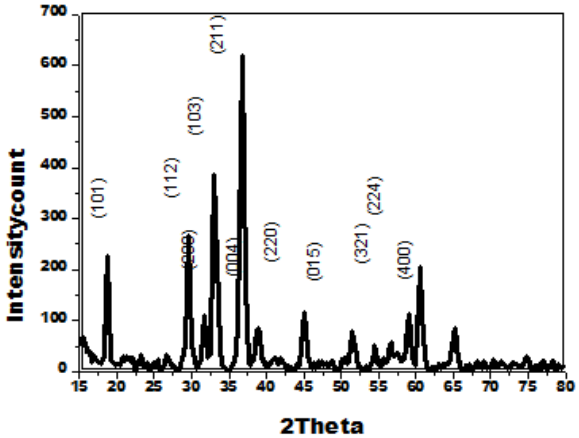

Fig. 2. XRD of Mn_3O_4 nanoparticles.

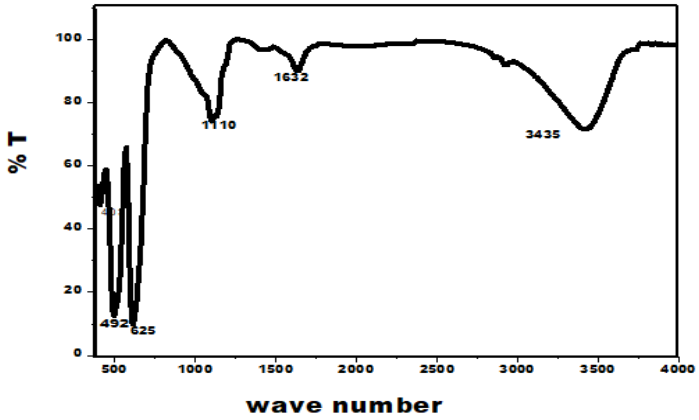

Fig. 3. FT-IR spectrum of the obtained Mn_3O_4 nanoparticle.

obtained. The broad band at 3436cm^{-1} is assigned to small amount of absorbed water in the sample [39]. For spinels, vibrations of ions in the crystal lattice are usually observed in the range 1000-400 cm^{-1} [40]. The vibrational frequency at 625 cm^{-1} corresponds to the intrinsic stretching vibrations of metal at the tetrahedral site, $M_{tetra} \leftrightarrow O$ where as the band stretching vibrations in the range 500-385 cm^{-1} account for octahedral metal stretching, $M_{Octa} \leftrightarrow O$ [41-42]. The peaks in the range 1084-1554 cm^{-1} corresponds to the vibration of O–H bonds connected with Mn atoms [39]. The strong peak at 625 cm^{-1} is characteristic of hausmannite with a spinel structure, corresponding to the Mn-O stretching vibration of divalent 'Mn' ions in the tetrahedral co-ordination. The other strong peak at 492 cm^{-1} corresponds to the Mn - O stretching vibration of Mn^{3+} ions in the octahedral co-ordination.

UV-Visible spectroscopy

UV-Visible absorption spectrum of Mn_3O_4 is given in Fig. 4. UV-Visible spectrum is usually used to obtain the band gap of semiconductor materials. The absorption bands at 226 and 353 nm are attributed to the allowed $O^{2-} \rightarrow Mn^{2+}$ and $O^{2-} \rightarrow Mn^{3+}$ charge transfer transitions respectively [43].This spectrum is typical of the hausmannite phase. From the Tauc's plot obtained by plotting hν against $(\alpha h\nu)^2$,

the band gap energies of the material were calculated and were found to be 2.4 eV and 2.9 eV as in Fig. 5 [44]. The low values of band gap energies suggest the application of the prepared material as a photo catalyst under visible light irradiation. Usually semiconductor metal oxides like CuO and ZnO show photocatalytic activities at UV region [45-46]. Structure modifications like formation of composites or mixed oxides shift the band gap energy to the visible range. Cui *et al.* in their studies on the evolution of hydrogen

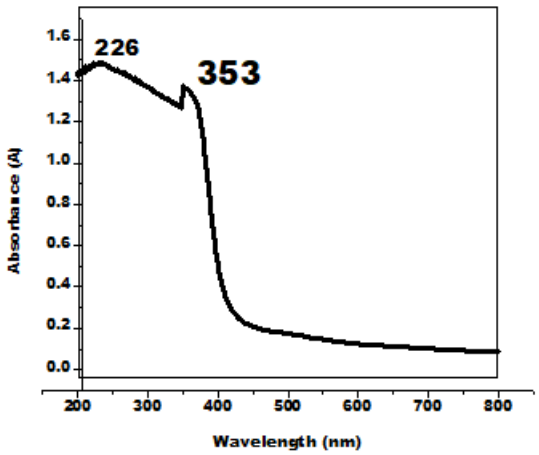

Fig. 4. UV-Visible spectrum.

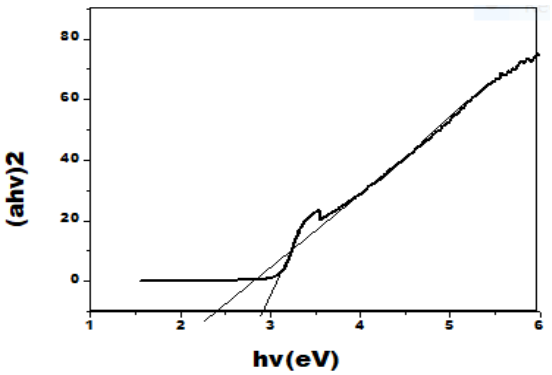

Fig. 5. Tauc's plot.

from aqueous solutions of Na_2S and Na_2SO_3, found that composite of $ZnIn_2S_4/K_2La_2Ti_3O_{10}$ has activity in the visible region whereas $K_2La_2Ti_3O_{10}$ alone has activity in the UV region [47, 48].

X-Ray photoelectron spectroscopy

Fig. 6 shows a typical X-ray photoelectron spectrum (XPS) of the as prepared Mn_3O_4 for Mn 2p region at room temperature. The binding energies of Mn ($2p_{3/2}$) and (Mn $2p_{1/2)}$ were found to be 641.7and 653.5eV respectively and agree well with the value reported in the literature [49, 50].In addition, the spin-orbital coupling between Mn $2p_{3/2}$ and Mn $2p_{1/2}$ can also be assigned to the oxides of Mn^{2+} and Mn^{3+} respectively [51, 52]. Therefore, XPS studies further support that the prepared material is Mn_3O_4 in the pure phase.

Scanning Electron Microscopy

The SEM image (Fig. 7) shows a well-defined morphology of nearly spherical shape for the prepared Mn_3O_4 nanoparticles. The EDX spectrum (Fig. 8) shows that the prepared compound contains only Mn and O as elements. It is also confirmed from the table (Table 1).

Transmission Electron Microscopy

TEM image shown in Fig. 9 reveals the presence of spherical particles of Mn_3O_4 with uniform morphology and having a particle size of 15 nm. The selected area electron diffraction (SAED) pattern in Fig. 10 shows that the particles are well crystallized. The diffraction rings on SAED image match with the peaks in XRD pattern which also proves the hausmannite structure for the prepared Mn_3O_4 nanoparticle.

Table 1. Elemental composition of Mn_3O_4 Nanoparticles.

Element	Line Type	Wt%
O	K Series	22.14
Mn	K Series	77.86
Total		100

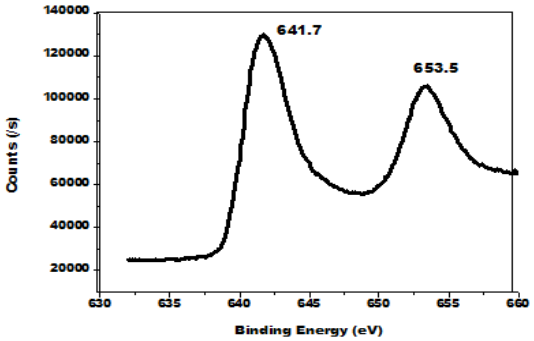

Fig. 6. XPS spectrum of the Mn 2p scan of Mn_3O_4 nanoparticle.

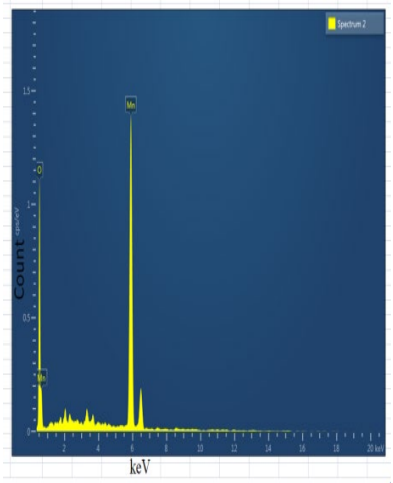

Fig. 8. EDX spectrum Mn_3O_4 nanoparticle.

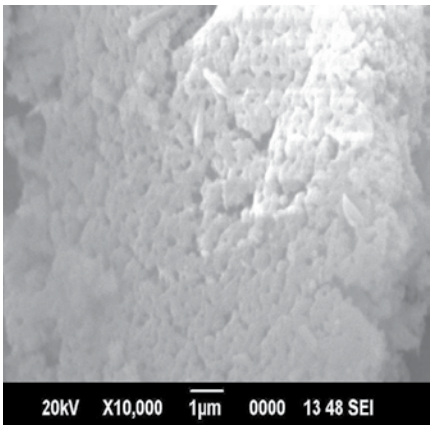

Fig. 7. SEM images of Mn_3O_4 nanoparticles.

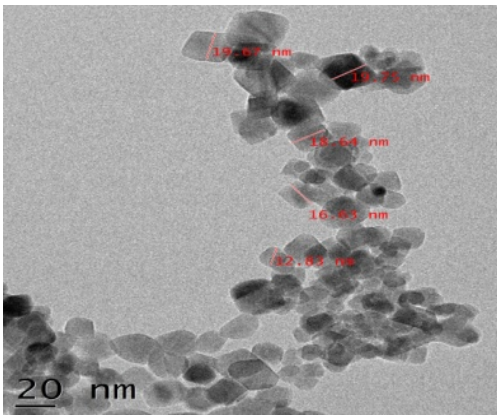

Fig. 9. TEM image of Mn_3O_4 nanoparticle.

Photo catalytic degradation of Malachite Green using Mn_3O_4.

The photocatalytic degradation of MG in aqueous solution using Mn_3O_4 catalyst was studied under visible light. MG is usually resistant to biodegradation and resists photolysis. The photocatalytic activity depends on many factors like crystallinity, band gap energy and morphology of the nanostructured material. The sequential absorption spectrum of MG aqueous solution under visible light illumination in the presence of Mn_3O_4 catalyst for different interval times (0 - 150 min) is shown in Fig. 11- 13. MG shows a strong characteristic absorption at 620 nm and the absorption maximum steadily decreases as the exposure time of visible light increases. The intense blue colour of the initial solution disappears gradually and becomes almost colourless as the irradiation time increases, indicating the degradation of the dye. Experiments were conducted at different concentrations of dye, different amounts of catalyst and varying pH.

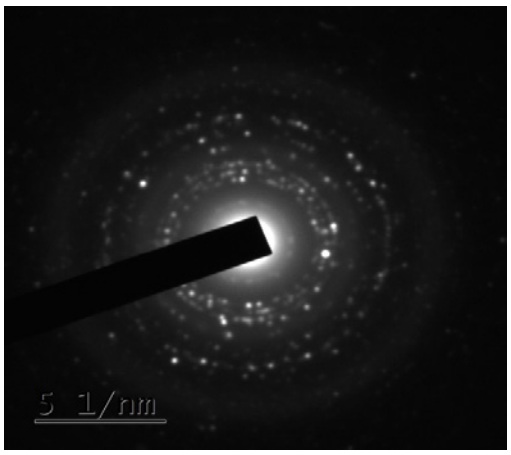

Fig.10. SAED pattern of Mn_3O_4.

Effect of Concentration of Malachite green Dye

The effect of concentration on the rate of dye degradation was studied by varying the concentration of dye from 10 to 40 ppm (Fig. 11(a) to 11(d)). It was seen that rate of dye degradation increased with increase in the initial concentration of MG up to 20 ppm, because of the fact that as the concentration of dye increased number of dye molecules also increased resulting in higher rate of reaction. There was a decrease in the rate of degradation with further increase in concentration (> 20 ppm) of dye. This may be due to the fact that at high concentration, the dye will act as an internal filter for the incident light.

Effect of Amount of Mn_3O_4

The effect of amount of nanophotocatalyst on the rate of dye degradation was examined by varying the amount of catalyst from 0.05 to 0.2 gm / 200ml of the dye solution (Fig. 12 (a) to 12(d)).It was observed that at lower dose of catalyst (0.05 to 0.1 gm), the rate of dye degradation increased rapidly with time. But at higher dose (0.15 to 0.2gm), the rate of dye degradation was found to decrease. The decreased degradation rate at higher catalyst dose is due to multilayer formation, which causes recombination of electron-hole pair with time.

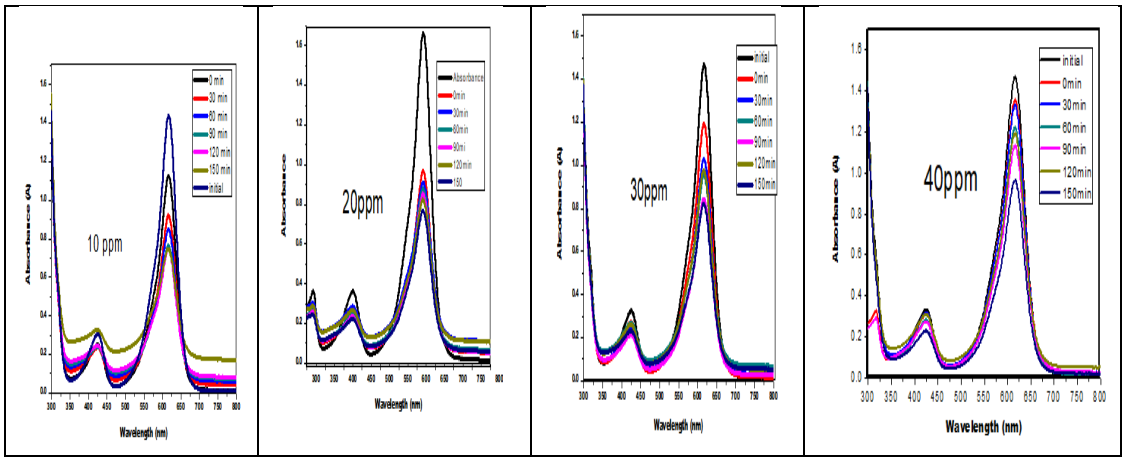

11(a) 11(b) 11(c) 11(d)

Fig. 11. Effect of concentration of malachite green dye on degradation with time.

Effect of pH

The rate of degradation of dye increased with increase in pH over the entire range studied from pH 4 to 9 (Fig. 13 (a) to 13(c)). An increase in the rate of photo catalytic degradation of malachite green with increase in pH may be due to the generation of more ·OH radicals, which are produced from the reaction between $^{-}$OH ions and hole (h^{+}) of the semiconductor nanoparticle. Above pH 9, the cationic form of malachite green converts to its natural form, which faces no attraction towards the negatively charged semiconductor surface due to adsorption of –OH ions [53].

The percentage of dye degradation (R %) was calculated using equation (1) and its variance with exposure to sunlight is shown in Fig. 14 (a) to 14 (c).

For 0.1 gm of the catalyst, the percentage degradation of dye increased with increase in concentration and reached a maximum (55%) at 20 ppm. For fixed concentration of dye (10 ppm), the percentage degradation increased with the dose of Mn_3O_4 and reached a maximum (60%) at 0.1gm. The percentage degradation also increased with increase in pH up to the value of pH 9 (78%).

Mechanism

On the basis of these observations a tentative mechanism for photo catalytic degradation of malachite green dye may be proposed as:

$$^{1}MG_{0} + hv \rightarrow {}^{1}MG_{1} \quad (2)$$

$$^{1}MG_{1} \rightarrow {}^{3}MG_{1} \quad (3)$$

$$Mn_3O_4 + hv \rightarrow e^{-}(CB) + h^{+}(VB) \quad (4)$$

$$e^{-} + O_2 \rightarrow O_2^{-} \quad (5)$$

$$O_2^{-} + {}^{3}MG1 \rightarrow \text{Leuco MG} \quad (6)$$

$$\text{Leuco MG} \rightarrow \text{End Products} \quad (7)$$

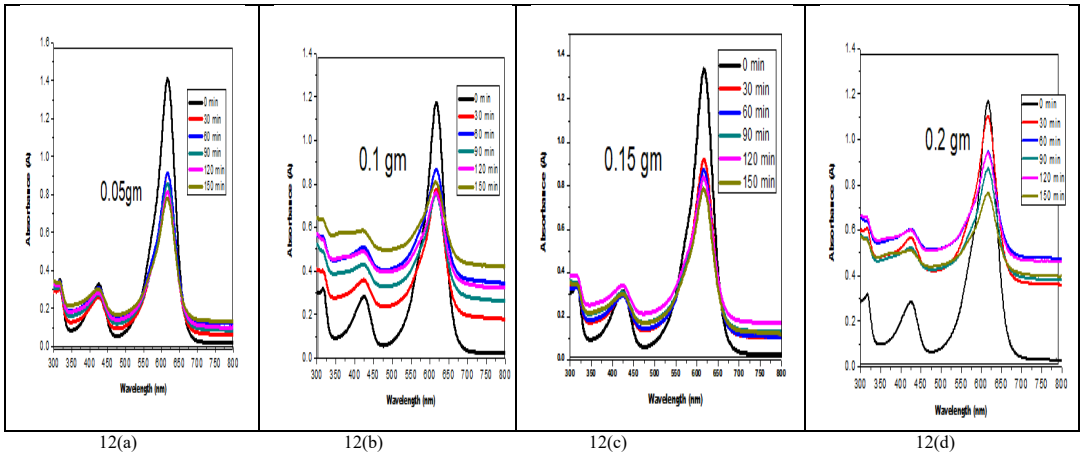

12(a) 12(b) 12(c) 12(d)

Fig. 12. Effect of amount adsorbent on dye degradation with time.

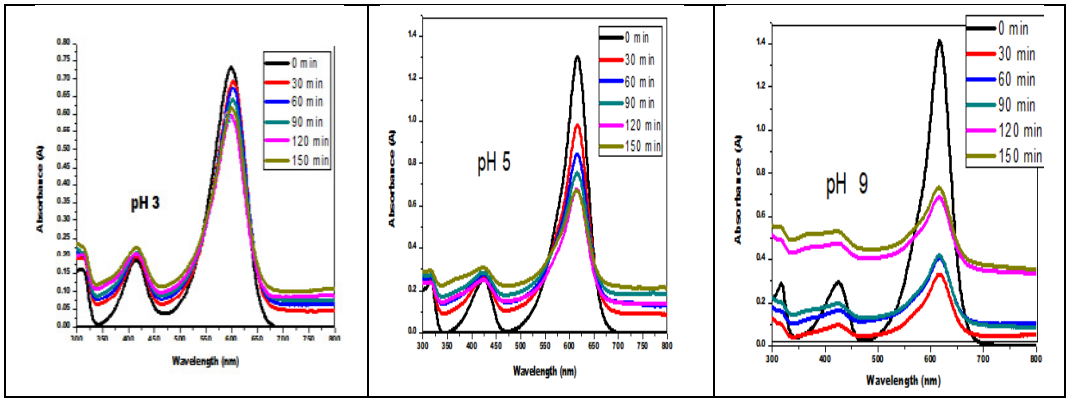

13(a) 13(b) 13(c)

Fig. 13. Effect of pH on dye degradation with time.

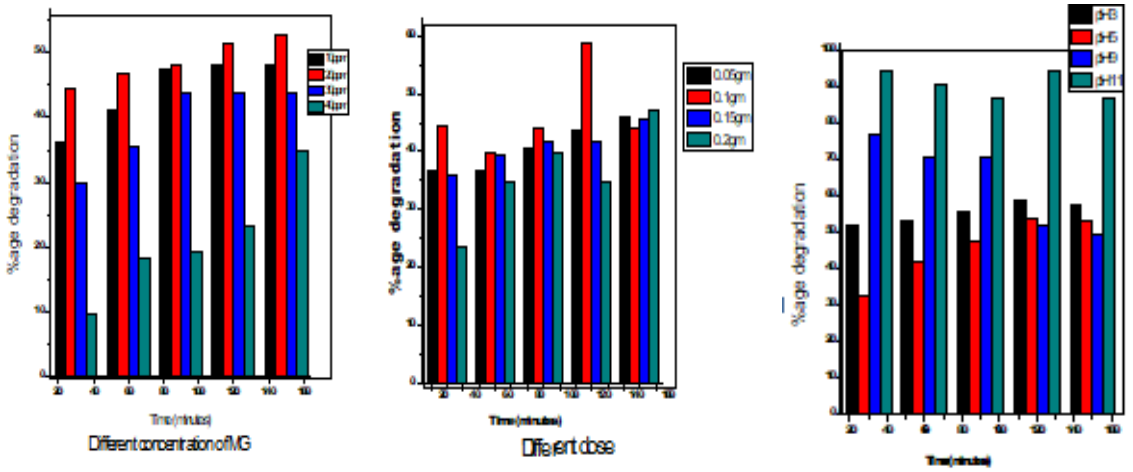

14(a) 14(b) 14(c)

Fig. 14. Percentage degradation of MG dye with time for various conditions like concentration of dye, amount of adsorbent and pH.

Malachite green (MG) absorbs radiations of suitable wavelength and gives rise to its first excited singlet state. Then it undergoes intersystem crossing (ISC) to give the triplet state of the dye. On the other hand, the semiconducting Mn_3O_4 also utilizes the radiant energy to excite its electron from valence band to the conduction band. This electron will be absorbed by oxygen molecule (dissolved oxygen) generating superoxide anion radical (O_2^{-}•). This anion radical will reduce the dye malachite green to its leuco form, which may ultimately degrade to end products. It was also confirmed that this degradation proceeds through reduction and not oxidation as the rate of degradation was not affected appreciably in presence of hydroxyl radical scavenger (2-propanol).

Studies on the degradation of dyes using semiconductor nanoparticles reported earlier from our laboratory were using UV light as irradiation source [45-46]. But the use of visible light is more advantages for environmental applications. Attempts have been made in this direction by various researchers. The photo degradation of Rhodamine B was successfully carried out using PbS sensitized $K_4Nb_6O_{17}$ nanocomposite by Cui *et al.* [11]. Recently, Rajendran et al reported the degradation of Methylene blue by PVA assisted Bi_2WO_6-CdS nanocomposite film under visible light irradiation [54]. Xiong et al conducted photocatalytic degradation of Rhodamine B over graphene-gold nanocomposite under visible light irradiation [55]. The biosynthesized Mn_3O_4 in the present study is a promising photo catalyst for the degradation of dyes like MG using visible light irradiation.

CONCLUSION

A simple, eco-friendly, non-toxic and environmentally efficient green method is explained for preparing Mn_3O_4 nanoparticles from Simarouba Glauca leaf extract. The XRD, FT-IR, UV-Visible and XPS spectral studies confirm the formation of pure tetragonal hausmannite (Mn_3O_4) spinel nanoparticles. The SEM and TEM studies suggest sphere like morphologies for the obtained Mn_3O_4 nanoparticles with an average particle size of 15 nm. The synthesized material is a good photo catalyst for the degradation of Malachite green dye. The optimum conditions for dye degradation are at pH 9 for 0.1 gm of the catalyst at 20ppm dye concentration. The results show the excellent photo catalytic performance of Mn_3O_4 assigned mainly to the formation of oxygen vacancies and mixed valence states of manganese. The above results suggest the potential applications of Mn_3O_4 in industrial waste water treatment.

ACKNOWLEDGEMENTS

One of the authors (G. Sreekala) is grateful to UGC, New Delhi for providing the financial assistance in the form of FDP. STIC-CUSAT and SICC, Kariavattom are also acknowledged for providing instrumental facilities.

CONFLICT OF INTEREST

The authors declare that they have no competing interests.

REFERENCES

[1] Rajeshkannan R., (2011), Decolourization of malachite green-optimization, isotherm and kinetic studies. *Chem. Ind. Chem. Eng.* 17: 67–79.

[2] Ali I., Al-Othman Z. A., Alwarthan A., (2016), Molecular uptake of congo red dye from water on iron composite nano particles. *J. Mol. Liq*. 224: 171–176.

[3] Khan T. A., Sharma S., Ali I., (2011), Adsorption of rhodamine B dye from aqueous solution onto acid activated mango (*Mangifera indica*) leaf powder: Equilibrium, kinetic and thermodynamic studies. *J. Toxicol. Environ. Health.* 3: 286–297.

[4] Ali I.,GuptaV. K., (2006), Advances in water treatment by adsorption technology. *Nat. Protoc*. 1: 2661-2667.

[5] Culp S. J., (2002), Mutagenicity and carcinogenicity in relation to DNA adduct formation in rats fed leucomalachite green. *Mutat. Res*. 506–507: 55–63.

[6] Chandran D., (2016), A review of the textile industries waste water treatment methodologies. *Int. J. Sci. Eng. Res*. 7: 2229–5518.

[7] Ali I., (2012), New generation adsorbents for water treatment. *Chem. Rev*. 112: 5073–5091.

[8] Ali I., Asim M., Khan T. A., (2017), Removal of chromium (VI) from aqueous solution using guar gum–nano zinc oxide biocomposites adsorbent. *Arab. J. Chem*. 10: 2388–2398.

[9] Ali I., (2014), Water treatment by adsorption columns: Evaluation at ground level. *Sep*. *Purif. Rev.* 43: 175–205.

[10] Khan T. A., Nazir M., Ali I., Kumar A, (2017), Removal of chromium (VI) from aqueous solution using guar gum–nano zinc oxide biocomposite adsorbent. *Arab. J. Chem*. 10: 2388-2398.

[11] Cui W, Shao M, Liu L, liang Y, Rana L., (2013), Enhanced visible-light-responsive photocatalytic property of PbS-sensitized $K_4Nb_6O_{17}$ nanocomposite photocatalysts. *Appl. Surf. Sci*. 276: 823–831.

[12] Balaji Anjaneyulu R., Sathish Mohan B., Parasuram Naidu G., Muralikrishna R., (2018), Visible light enhanced photocatalytic degradation of Methylene blue by ternary nanocomposite. MoO_3/Fe_2O_3/rGO. *J. Asian Ceram. Soc.* 6: 183-195.

[13] Balu S., Uma K., Pan G. T., Thomas C.-K., Yang T. C. K., Ramaraj S. K., (2018), Degradation of Methylene Blue dye in the presence of visible light using SiO_2@α-Fe_2O_3 nanocomposites deposited on SnS_2 flowers. *Materials.* 11: 1030-1036.

[14] Armstrong A. R., Bruce P. G., (1996), Synthesis of layered $LiMnO_2$ as an electrode for rechargeable lithium batteries. *Nature*. 381: 499-500.

[15] Mohan G. R., Ravinder D., Ramana Reddy A. V., Boyanov B. S., (1999), Dielectric properties of polycrystalline mixed nickel-zinc ferrites. *Mater. Lett.* 40: 39–45.

[16] Buckelew A., Gal´an-Mascar J. R., Dunbar K. R., (2002), Facile conversion of the face- centered cubic prussian-blue material $K_2[Mn_2(CN)_6]$ into the spinel oxide Mn_3O_4 at the solid/water interface. *Adv. Mater.* 14: 1646-1648.

[17] Myung S. T., Komaba S., Kumagai N., (2002), Hydrothermal synthesis and electrochemical behavior of orthorhombic $LiMnO_2$. *Electrochim. Acta.* 47: 3287–3295.

[18] Grootendorst E. J., Verbeek Y., Ponec V., (1995), The role of the mars and van krevelen mechanism in the selective oxidation of nitrosobenzene and the deoxygenation of nitrobenzene on oxidic catalysts. *J. Catal.* 157: 706–712.

[19] Stobbe E. R., De Boer B. A., Geus J. W., (1999), The reduction and oxidation behaviour of manganese oxides. *Catal. Today.* 47: 161–167.

[20] Kijlstra W., Daamen J., Vandegraaf J., Vanderlinden B., Poels E., Bliek A., (1996), Inhibiting an deactivating effects of water on the selective catalytic reduction of nitric oxide with ammonia over MnO_x/Al_2O_3. *Appl. Catal. B: Environ.* 7: 337–357.

[21] Mendelovici E., Sagarzazu A., (1988), Thermal synthesis of hausmanite via manganese Alkoxide. *Thermochim. Acta.* 133: 93–100.

[22] Finocchio E., Busca G., (2001), Characterization and hydrocarbon oxidation activity of coprecipitated mixed oxides Mn_3O_4/Al_2O_3. *Catal. Today*. 70: 213–225.

[23] Demazeau G., (1999), Solvothermal processes: A route to the stabilization of new Materials. *J. Mater. Chem.* 9: 15–18.

[24] Yang L. X., Zhu Y. J., Tong H., Wang W. W., Cheng G. F., (2006), Low temperature synthesis of Mn_3O_4 polyhedral nanocrystals and magneticstudy. *J. Solid State Chem*. 179: 1225–1229.

[25] Salavati-Niasari M., Davar F., Mazaheri M., (2008), Synthesis of Mn_3O_4 nanoparticles by thermal decomposition of a [bis(salicylidiminato) manganese (II)] complex. *Polyhedron.* 27: 3467-3471.

[26] Chang Y. Q.,Yu D. P., Long Y., Xu J., Luo R., Ye C., (2005), Large-scale fabrication of single-crystalline Mn_3O_4 nanowires via vapor phase growth. *J. Crystal Growth.* 279: 88–92.

[27] Du J., Gao Y., Chai L., Zou G., Li Y., Qian Y., (2006), Hausmannite Mn_3O_4 nanorods: Synthesis, characterization and magnetic properties. *Nanotechnol.* 17: 4923–4928.

[28] Gopalakrishnan I. K., Bagkar N., Ganguly R., Kulshreshtha S. K., (2005), Synthesis of super paramagnetic Mn_3O_4 nanocrystallites by ultrasonic irradiation. *J. Crystal Growth.* 280: 436–441.

[29] Hu Y., Chen J., Xue X., Li T., (2006), Synthesis of monodispersed single-crystal compass-shaped Mn_3O_4 viagamma-rayirradiation. *Mater. Lett.* 60: 383–385.

[30] Ozkaya T., (2008), *Master thesis*, Fatih University, Istanbul, Turkey.

[31] Sharanya V. K., Gayathiri K., Sangeetha M., Shyam P. G., Gopi S. K., Vimalavathini R., Kavimani S., (2016), A pharmacological review on simarouba glauca DC. *Int. J. Pharma. Res. Rev.* 5: 32-36.

[32] Ghahi A., (1990), Introduction to pharmacognosy, Ahmadu Bello University press, Ltd.Zaria, Nigeria, 45-47.

[33] Patil M. S., Gaikwad D. K., (2011), A critical review on medicinally important oil yielding plant Laxmitaru (*Simarouba glauca* DC.). *J. Pharm. Sci. Res*. 3: 1195-1213.

[34] Sugimogo M., (1999), Past, present & future of ferrites. *J. Am. Ceram. Soc.* 82: 269–280.

[35] Fritsch A. S., Sarrias J., Rousset A., Kulkarni G. U., (1998), Low-temperature oxidation of Mn_3O_4 hausmannite. *Mat. Res. Bull*. 33: 1185–1194.

[36] Ozkaya T., Baykal A., Kavas H., Koseglu Y., Topark M. S., (2008), A novel synthetic route to Mn_3O_4 nanoparticles and their magnetic evaluation. *Physica B*. 403: 3760-3764.

[37] Santra S., Tapec R., Theodoropoulou N., Dobson J., Hebard A., Tan W., (2001), Synthesis and characterization of silica-coated Iron Oxide nanoparticles in microemulsion: The effect of nonionic surfactants. *Langmuir*. 17: 2900-2906.

[38] Patil K. C, Aruna S., Mimani T., (2002), Combustion synthesis: An update. *Current Opin. Solid State Mater. Sci.* 6: 507-512.

[39] Ananth M. V., Pethkar S., Dakshinamurthi K., (1998), Distortion of MnO_6 octahedra and electrochemical activity of Nstutite-based MnO_2 polymorphs for alkaline electrolytes an FTIR study. *J. Power Sources.* 75: 278-282.

[40] Brabers V. A. M., (1969), Infrared spectra of cubic and tetragonal manganese ferrites. *Phys. Status Solidi*. 33: 563-572.

[41] Durmu S., Kavas Z., Baykal H., Toprak A., (2009), A green chemical route for the synthesis of Mn_3O_4 nanoparticles. *Cent. Eur. J. Chem*. 7: 555-559.

[42] Durmus Z., Tomas M., Baykal A., Kavas H., Altınçekiç T. G., Toprak M. S., (2010), The effect of neutralizing agent on the synthesis and characterization of Mn_3O_4 nanoparticles. *Russ. J. Inorg. Chem*. 55: 1947-1952.

[43] Boyero Macstre J., Fernandez Lopez E., Gallardo-Amores J. M., Ruano Casero R., (2001), Influence of the synthesis parameters on the structural and textural properties of precipitated manganese oxide. *Int. J. Inorg. Mater.* 3: 889-899.

[44] Dubal D. P., Dhawale D. S., Pawar S. M., (2010), A novel chemical synthesis and characterization of Mn_3O_4 thin films for supercapacitor application. *Appl. Surf. Sci.* 256: 4411-4416.

[45] Rejani P., Radhakrishnan A., Beena B., (2014), Photo catalytic decomposition of malachite green in aqueous solutions under UV irradiation using nano ZnO Rod. *Iranica J. Energy Envir.* 5: 233-239.

[46] Radhakrishnan A., Padmavathi R., Beena B., (2018), CuO nano structures as an ecofriendly nano photo catalyst and antimicrobial agent for environmental remediation. *Int. J. Nano Dimens.* 9: 145-157.

[47] Cui W., Guo D., Liu L., Hu J., Ranab D., Liang Y., (2014), Preparation of $ZnIn_2S_4/K_2La_2Ti_3O_{10}$ composites and their photocatalytic H_2 evolution from aqueous Na_2S/Na_2SO_3 under visible light irradiation. *Catal. Commun.* 48: 55–59.

[48] Cui W., Qia Y., Li Liu L., Ranab D., Hu J., Liang Y., (2012), Synthesis of $PbS–K_2La_2Ti_3O_{10}$ composite and its photocatalytic activity for hydrogen production. *Prog. Nat. Sci: Mater. Int.* 22: 120–125.

[49] Wager C., Riggs W., Davia L., Moulder J., Muilenber G., (1979), Handbook of X-ray photoelectron spectroscopy, Perkin Elmer Corporation physical electronic division, waltham, MA.

[50] Wang W., Ao L., (2008), Synthesis and optical properties of Mn_3O_4 nanowires by decomposing $MnCO_3$ nanoparticles in flux. *Crys. Growth and Design.* 8: 358-362.

[51] Davar F., Salavati-Niasari M., Mir N., Saberyan K., Monemzadeh M., Ahmadi E., (2010), Thermal decomposition route for synthesis of Mn_3O_4 nanoparticles in presence of a novel Precursor. *Polyhedron.* 29: 1747–1753.

[52] Salavati-Niasari M., Davar F., Mazaheri M., (2008), Synthesis of Mn_3O_4 nanoparticles by thermal decomposition of a [bis (salicylidiminato)manganese(II)] complex. *Polyhedron.* 27: 3467–3471.

[53] Ameta K. L., Neema P., Rakshit A., (2014), Synthesis, characterisation and use of novel bimetal oxide catalyst for photoassissted degradation of Malachite green dye. *J. Mater.* 2014: 1-5.

[54] Ranjith R., Krishnakumar V., Venkatesan J., Boobas S., Jayaprakash J., (2018), Photocatalytic degradation of metronidazole and methylene blue by PVA-assisted Bi_2WO_6–CdS nanocomposite film under visible light irradiation. *Appl. Nanosc.* 8: 61–78.

[55] Zhigang X., Li Zh., Jizhen M., Zhao X. S., (2010), Photocatalytic degradation of dyes over graphene–gold nanocomposites under visible light irradiation. *Chem. Commun*. 46: 6099–6101.